2009 International Workshop on Nonlinear Circuits and Signal Processing
NCSP'09, Waikiki, Hawaii, March 1-3, 2009

A CMOS Frequency Comparator based on Jamming Avoidance Response of *Eigenmannia*

Daichi Fujita†, Tetsuya Asai, and Yoshihito Amemiya

Graduate School of Information Science and Technology, Hokkaido University.
Kita 14, Nishi 9, Kita-ku, Sapporo, 060-0814 Japan.
Phone:+81-11-706-7147, Fax:+81-11-706-7890
† email: fujita@lalsie.ist.hokudai.ac.jp

Abstract

In this paper, we implement a model of an electric fish, *Eigenmannia*, that detects frequency differences between the individuals, on analog CMOS circuits. The circuit's fundamental function is equivalent to a conventional CMOS frequency comparator, although less post-processing is still required. The circuit consists of P- and T-units each of which encodes amplitudes and phases of the monitored electronic signals, respectively. Using a simulation program of integrated circuit emphasis (SPICE), we demonstrate that the proposed circuit can detect the phase difference effectively.

1. Introduction

Eigenmannia is an electric fish that generates sinusoidal (AC) voltages at their electric organ (electric organ discharge: EOD) to recognize the surrounding environment. Electroreceptors on their skin surface detect the local electromagnetic field, to recognize "obstacles" around the fish. Because local obstacles interfere with the electromagnetic field, by comparing the interfered field (phases and amplitudes of detected voltages) with less-interfered ones, *Eigenmannia* can recognize the surrounding environment, *e.g.*, positions and shapes of the obstacles, which results in their intelligent electrolocation ability.

When two individuals (fishes) each of which emits the same EOD frequencies are nearly located, they shift their EOD frequencies away from each other, because the electrolocation ability is vulnerable to interference with the fish's own EODs. This behavior is called *jamming-avoidance response* (JAR). To do this, *Eigenmannia* discriminates a sign of the frequency difference between their own EOD and the neighbor's one [1].

In this paper, we implement a model of JAR in *Eigenmannia* on analog CMOS circuits to build fundamental circuits for a frequency comparator that would be useful in low-power wireless communication systems, aiming at possible applications to frequency hopping, automatic channel scanning in Wi-Fi systems, and so on.

2. Brief Review of Model of JAR in *Eigenmannia*

The primary purpose of JAR in *Eigenmannia* is to avoid generating the same EODs among them by increasing (or decreasing) their EOD frequencies. Let us assume that two fishes, which we denote F1 and F2, are nearly located, and that they have almost the same EOD frequencies ($f_1 \approx f_2$). Firstly, F1 calculates the frequency difference ($\Delta f_{21} \equiv f_2 - f_1$), whereas F2 does $\Delta f_{12} \equiv f_1 - f_2$. To avoid having the same EOD frequencies, F1 decreases (or increases) f_1 when $\Delta f_{21} > 0$ (or $\Delta f_{21} < 0$), *i.e.*, F1's EOD frequency is lower (or higher) than that of F2. Similarly, F2 decreases (or increases) f_2 when $\Delta f_{12} > 0$ (or $\Delta f_{12} < 0$), *i.e.*, EOD frequencies of F2 is lower (or higher) than that of F1.

Now let us see how F1 and F2 compare their EOD frequencies. Assume that F1 and F2 are nearly located in parallel. They accept interfered EODs and less-interfered (self-generated) EODs via two electroreceptors located at different body positions, *e.g.*, positions A and B shown in Fig. 1(a). Now assume that Fig. 1(a) represents F1's body placement. The solid arrows represent F1's EODs, while dashed ones represents EODs generated by F2. Because F1's EOD passes along F1's skin surface, signals detected by the electroreceptors at A are almost the same as signals at B. On the other hand, EODs generated by F2 would pass through F1's trunk perpendicularly. Therefore, signals detected by the electroreceptors at A are different from signals at B.

F1 accepts synthesized EODs of F1's own EODs (S_1) and F2's ones (S_2) at electroreceptors on A and B. We denote the synthesized EODs on A and B as $S_{\rm A}$ and $S_{\rm B}$, respectively. Figure 1(b) shows the EODs ($S_{\rm A}$ and $S_{\rm B}$) detected by electroreceptors on A and B as well as S_1 and S_2. In this figure, we assume that S_1's frequency (f_1) is lower than that of S_2 (f_2), *i.e.*, $\Delta f_{21} > 0$. F1 selects largely interfered EODs among $S_{\rm A}$ and $S_{\rm B}$ ($= S_{\rm A}$ in this example), and then extracts the amplitude information. A P-unit, one kind of electroreceptors on *Eigenmannia*'s skin, encodes the amplitudes in spike densities, as shown in Fig. 1(c) bottom. The mean-firing rate of a P-unit represents the amplitudes of the synthesized EODs ($S_{\rm A}$). On the other hand, a T-unit, the other kind of electroreceptors on *Eigenmannia*'s skin, encodes the

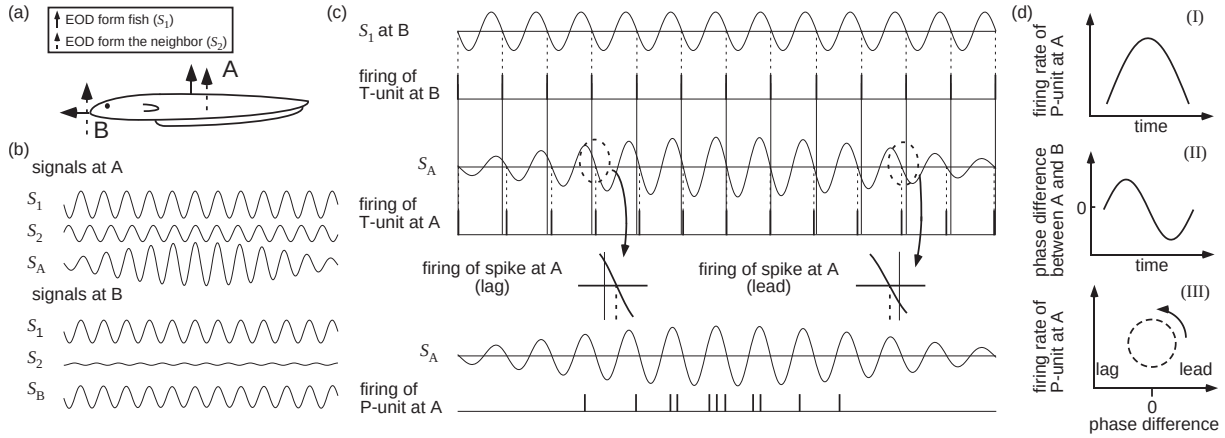

Figure 1: Model of jamming-avoidance response (JAR) in *Eigenmannia*.

phase difference between the synthesized EODs at A and B. As shown in Fig. 1(c) top, a T-unit fires only when the synthesized EODs have a certain phase ($= \pi(2n+1)$, n: integer). By calculating inter-spike intervals between the firing of the T-units on A and B, F1 extracts the phase information. Figures 1(d)-I and II show time courses of the normalized maximal firing rates of the P unit on A ($\equiv |S_{\rm A}|$) and normalized inter-spike intervals of the T units on A and B, respectively, within a given period of the synthesized EODs. When $|S_{\rm A}|$ and the phase difference are plotted in a 2-D plane, a circular trajectory appears, as shown in Fig. 1(c)-III. Directions of the rotation reflect the sign of Δf_{21}: clockwise for negative and counterclockwise for positive Δf_{21}. By detecting the direction, *Eigenmannia* makes a decision to increase or decrease their own EOD frequency [1].

3. Circuit Implementation of P- and T-units

Figure 2 shows the proposed P- and T-unit circuits. The P-cell circuit was designed based on the Volterra system [2]. Let us assume that $V_{\rm m}$ and $I_{\rm m}$ of the P-unit circuit, shown in Fig. 2(a), are zero at the initial state. The P-unit accepts $I_{\rm in}$, and the current is mirrored to node $V_{\rm m}$ via current mirror $\rm M_{P1}$-$\rm M_{P2}$. The current is integrated by the gate capacitance of $\rm M_{P3}$, which results in nonzero $V_{\rm m}$ as long as $I_{\rm ref} < I_{\rm in}$. The nonzero $V_{\rm m}$ induces drain currents of $\rm M_{P3}$, and the current is mirrored to $I_{\rm m}$ via current mirrors $\rm M_{P4}$-$\rm M_{P5}$ and $\rm M_{P6}$-$\rm M_{P7}$, which leads to the generation of nonzero $I_{\rm m}$. Therefore, $V_{\rm m}$ starts decreasing to zero because of the nonzero $I_{\rm m}$, which results in the decrease of $I_{\rm m}$. This operation is repeated as long as nonzero $I_{\rm in}$ is given. We regard the increase and decrease of $I_{\rm m}$ as output spikes because the number of the output spike is proportional to $I_{\rm in}$ within a certain current range. The output spikes are read out by $\rm M_{P8}$ as $I_{\rm Pout}$

Figure 2(b) illustrates the T-unit circuit. When $I_{\rm in} = 0$,

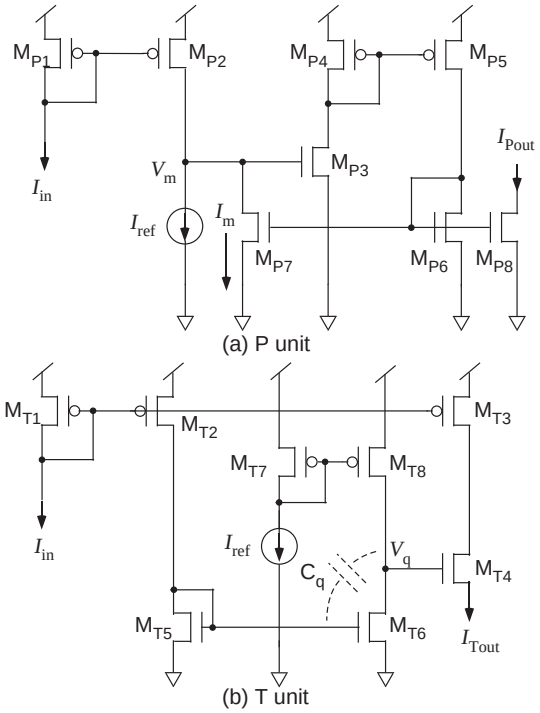

Figure 2: Analog CMOS circuits for P- and T-units.

$V_{\rm q}$ is high at the equilibrium ($\rm M_{T4}$ is thus turned on) because $I_{\rm in}$ ($= 0$) is mirrored to node $V_{\rm q}$ via current mirrors $\rm M_{T1}$-$\rm M_{T2}$ and $\rm M_{T5}$-$\rm M_{T6}$, and current mirror $\rm M_{T7}$-$\rm M_{T8}$ is biased by nonzero $I_{\rm ref}$. Therefore, when the T-unit circuit accepts nonzero $I_{\rm in}$, $I_{\rm in}$ is simply mirrored to the output terminal as $I_{\rm Tout}$. Because $\rm M_{T6}$ and $\rm M_{T8}$ can be regarded as a nMOS source-common amplifier ($\rm M_{T8}$ acts as the load), parasitic capacitance $\rm C_q$ of $\rm M_{T6}$ is amplified due to the Mirror effect. Once nonzero $I_{\rm in}$ was given, $V_{\rm q}$ is decreased because $\rm C_q$ is

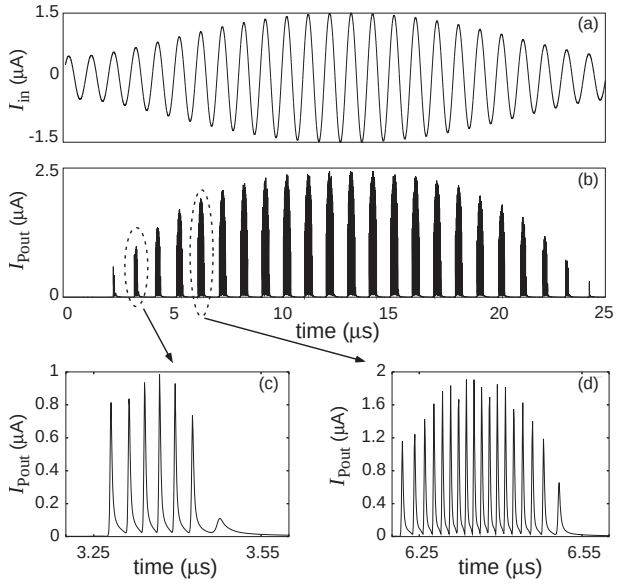

Figure 3: Raw spike outputs of P-unit circuit.

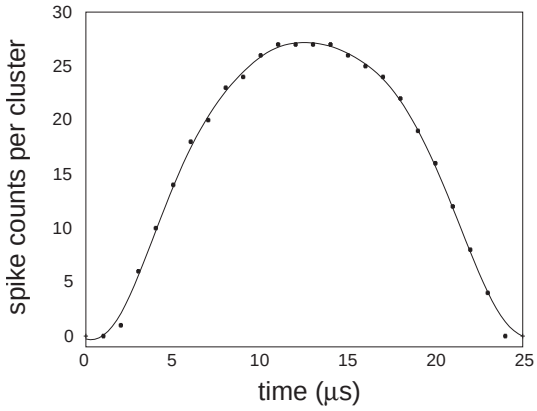

Figure 4: Spike counts within EOD period.

discharged by the current of M_{T6} (=I_{in}). Therefore, M_{T4} is gradually turned off, and consequently, I_{in} is not mirrored to the output terminal ($I_{Tout} \rightarrow 0$). This operation is equivalent to detecting rectified temporal deviations of I_{in}, which result in detection of a certain phase for periodic I_{in}.

4. SPICE Simulation Results

In the following simulations, we used TSMC 0.35-μm typical CMOS parameters. The power supply voltage was set at 3 V. Figure 3 shows simulation results of the P-cell circuit. We assumed two fishes (F1 and F2) generated their own EODs (S_1 and S_2) as

$$S_1 = \sin(2\pi f_1 t), \quad (1)$$

$$S_2 = \sin(2\pi f_2 t), \quad (2)$$

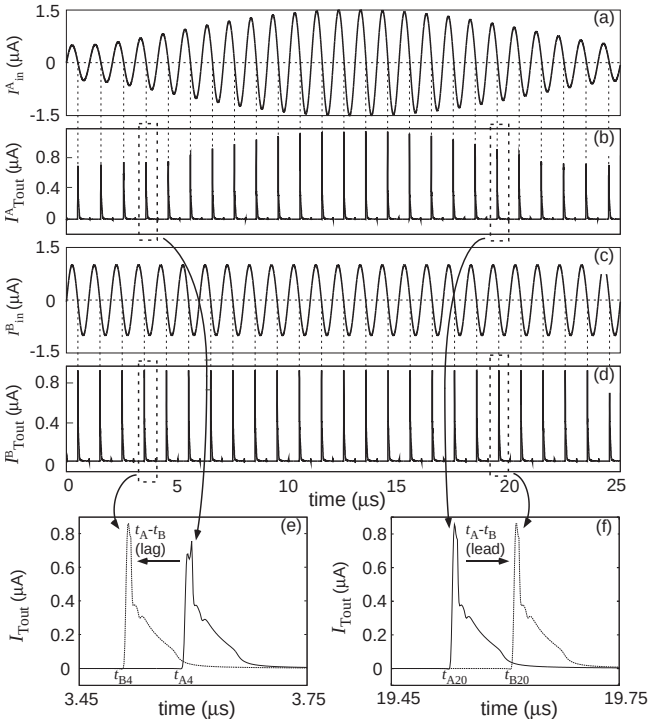

Figure 5: Raw spike outputs of T-unit circuit.

where f_1 and f_2 were set at 1 MHz and 1.04 MHz, respectively ($\Delta f_{21} > 0$). F1 accepts interfered input I_{in} as

$$I_{in} = I_0 S_1 + I_1 S_2, \quad (3)$$

where I_0 and I_1 were set at 1 μA and 0.5 μA, respectively, to emulate the interference. Figure 3(a) shows the interfered input current (I_{in}). Outputs of the P-cell circuit (I_{Pout}) are shown in Fig. 3(b) where I_{ref} of was set at 0.54 μA. Spike clusters in the dashed ellipses in the figure are enlarged in Figs. 3(c) and (d). Figure 4 shows the number of spikes (spike counts) versus time having the same time scale in Fig. 3(a), which indicated that the spike counts per each cluster was increased (or decreased) when the amplitudes of I_{in} was high (or low), *i.e.*, pulse-density modulation required for P-cell operations is realized by the proposed P-cell circuit.

Figure 5 shows simulation results of the T-cell circuit. We used two T-cell circuits corresponding T-cells of F1 on positions A and B in Fig. 1(a). Bias current I_{ref} of each T-cell circuit was set at 0.1 μA. Figures 5(a) and (c) show the interfered input current detected at A ($\equiv I_{in}^A = I_0 S_1 + I_1 S_2$) and no-interfered current detected at B ($\equiv I_{in}^B = I_0 S_1$), respectively. Outputs of the T-cells (I_{Tout}^A and I_{Tout}^B) were plotted in Figs. 5(b) and (d), which represented that the output spikes were generated only when the input current had a certain phase ($\approx \pi(2n+1)$, n: integer). Figures 5(e) and (f) shows enlarged spike clusters in dashed rectangles in Figs. 5(b) and

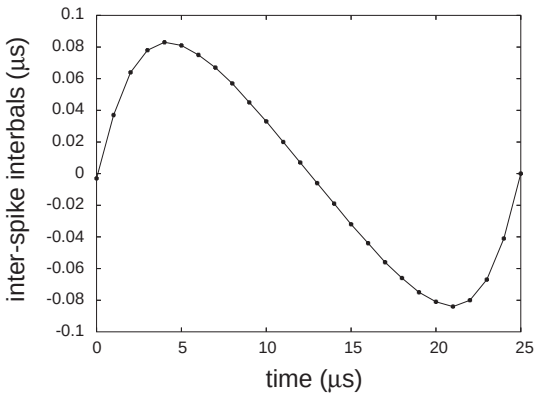

Figure 6: Inter-spike intervals within EOD period.

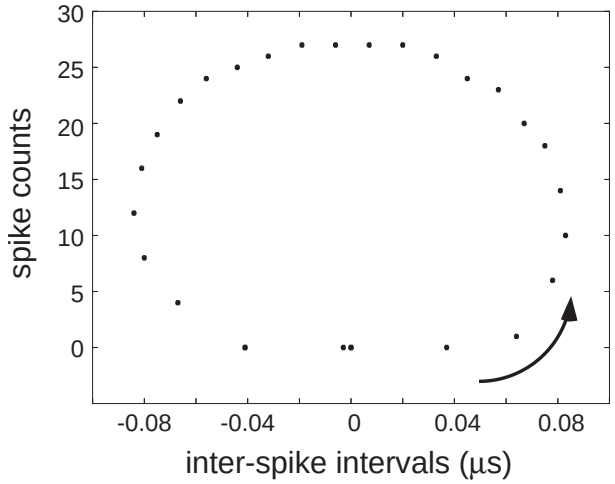

Figure 7: Spike counts detected by P-cell circuit versus inter-spike intervals calculated from two T-cells ($\Delta f_{21} > 0$).

(d). The inter-spike intervals, *i.e.*, $t_{\rm A} - t_{\rm B}$ in Figs. 5(e) and (f), were calculated at every n, and output spikes at $n = 4$ and 20 were plotted in the figures. Figure 6 shows the inter-spike intervals versus time having the same time scale in Figs. 5(a) to (d). The positive (or negative) intervals represent that the phase is lagged (or led).

Now let us see the operations of frequency comparison between S_1 and S_2, by integrating the outputs of the P- and T-cell circuits. Figure 7 plots spike counts in Fig. 4 versus inter-spike intervals in Fig. 6. As time increases, the plot (black circles) rotated on the 2-D plane counterclockwise, and the orbit draw a closed ellipse, which indicated $\Delta f_{21} > 0$, as explained in Sec. 2. Indeed, Δf_{21} was set at 40 kHz (> 0) in our setups. In contrast, when f_1 and f_2 were set at 1 MHz and 0.96 MHz ($\Delta f_{21} < 0$), respectively, the plot rotated on the plane clockwise, as shown in Fig. 8. Therefore, by integrating outputs of P- and T-cell circuits, one can discriminate the sign of the frequency difference by the rotating direction.

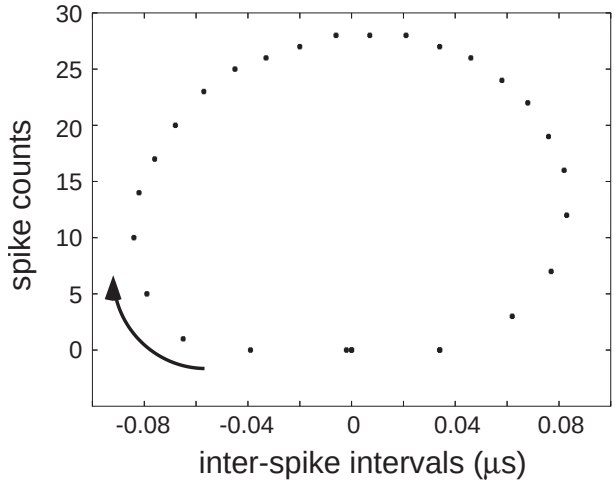

Figure 8: Clockwise rotation representing $\Delta f_{21} < 0$.

5. Conclusion

We designed fundamental circuits for a frequency comparator, *i.e.*, P- and T-cell circuits, based on a model of jamming-avoidance response in *Eigenmannia*. The P-cell circuit encodes amplitudes of input currents in spike density, whereas the T-cell circuit detects a certain phase of periodic input currents. Each circuit consisted of 8 transistors. Through SPICE simulations, we demonstrated that the circuit produced the expected responses described in [1].

To detect the frequency difference, some additional circuits are required, *i.e.*, i) circuits that plot the spike counts detected by P-cell circuit versus inter-spike intervals calculated from two T-cells and ii) circuits that determine the rotating direction from the outputs of i). A possible neural network model is proposed in [1], so we are going to implement the network, aiming at the implementation of a bio-inspired frequency comparator.

Acknowledgments

This study was supported by a Grant-in-Aid for Scientific Research on Innovative Areas [20111004] from the Ministry of Education, Culture Sports, Science and Technology (MEXT) of Japan.

References

[1] W. Heiligenberg, *Neural Nets in Electric Fish*, The MIT press, Cambridge, 1991.

[2] T. Asai, Y. Kanazawa, and Y. Amemiya, "A subthreshold MOS neuron circuit based on the Volterra system," *IEEE Trans. Neural Networks*, Vol. 14, No. 5, pp. 1308-1312 (2003).